CrystEngComm

Accepted Manuscript

ROYAL SOCIETY OF CHEMISTRY

www.rsc.org/crystengcomm

Amorphous Precursor Compounds for $CuInSe_2$ Particles Prepared by a Microwave-Enhanced Aqueous Synthesis and Its Electrophoretic Deposition

Delele Worku Ayele,[1] *Wei-Nien Su,*[2,*] *Chih-Chung Wu,*[1] *Ching-Yeh Shiau*[1] *and Bing–Joe Hwang*[1, 3*]

[1]*Department of Chemical Engineering National Taiwan University of Science and Technology, Taipei, 106, Taiwan*

[2]*Graduate Institute of Applied Science and Technology, National Taiwan University of Science and Technology, Taipei 106, Taiwan*

[3]*National Synchrotron Radiation Research Center Hsinchu 300, Taiwan*

Corresponding authors: wsu@mail.ntusdt.edu.tw; bjh@mail.ntust.edu.tw

Abstract

Amorphous precursor compounds for $CuInSe_2$ particles and films are prepared using a microwave enhanced method in aqueous solution. In this simple and rapid reaction, the precursor compounds with uniform morphology and amorphous phase were synthesized under microwave heating at 180 °C for 30 mins and pH value of 5. This amorphous compound is used as a precursor for the preparation of pure chalcopyrite $CuInSe_2$ particles by post reduction process. Post reduction processes were carried out in the presence of selenium powder in Ar (2% H_2-98% Ar) atmosphere at different temperature (300 °C, 400 °C & 500 °C) for 3 hrs. We find that this pure chalcopyrite $CuInSe_2$ particles prepared (at 500 °C) in this approach are suitable for the formation of uniform, crystalline and dense $CuInSe_2$ thin film for further application in solar cells. A pure, porous and uniform $CuInSe_2$ films were obtained using electrophoretic deposition techniques followed by annealing. The as-prepared amorphous precursor compounds and chalcopyrite $CuInSe_2$ particles are characterized by XRD, SEM, EDX elemental analysis and ICP.

Keywords: precursor compounds, amorphous, microwave, post reduction, $CuInSe_2$, electrophoretic deposition.

1. Introduction

The three important requirements of a photovoltaic device for large-scale terrestrial use are low cost, good efficiency, and stability.[1] The chalcopyrite semiconductor $CuInSe_2$ of the I-III-VI_2 families with superior properties such as its suitable direct band gap, high absorption coefficient, low cost and possibility either n-and p-type conductivity have attracted a great deal of interest as regards for possible photovoltaic application.[2-5] Solar cells based on chalcopyrite material with theoretical solar cell conversion efficiency of 27-32% have been predicted [6] and up to now photovoltaic device of $CuInSe_2$ with solar cell conversion efficiency of 19.6% have been reported.[7] The device performance of $CuInSe_2$ based solar cell largely depends on the quality and the properties of $CuInSe_2$ particles, which in turn directly relate to its methods and condition of preparation.

In the past years, several methods have been employed to prepare $CuInSe_2$ particles such as electrodeposition,[8] spray pyrolysis,[9, 10] sputtering[11] co-evaporation,[12] selenization,[13] solid-state reaction involving pure metal powders by microwave heating[14] and some other techniques.[15] However, in almost all of these methods, it is difficult to maintain satisfactory stoichiometry as well as to improve their morphology and crystallinity with lower temperature and pressure.[16]

Since the shape, size, and dimensionality of chalcopyrite materials are vital parameters for their properties,[17] developing a suitable method to synthesize $CuInSe_2$ materials with better stoichiometry and morphology is of interest and importance for their further application.[18] Synthesis of nanoparticles in aqueous solution has some particular advantages, because the method is economical, simple to operate, and environment-friendly.[19-21] However, this method requires longer reaction time, high temperature and difficulty to control the particle size via traditional heating**.** Within the past few years, it has been suggested that microwave (MW) irradiation is used to improve the drawbacks of hydrothermal routes with advantages such as shorter reaction time, increased product yields, lower cost, and higher purity of products as a result of reduced unwanted side reactions and so on.[22-25]

Consequently, it is anticipated to synthesize the semiconductor first into an amorphous precursor with desired composition via a microwave-assisted route. The obtained precursor powder can be further processed to the absorber layer for thin film solar cells by employing techniques like electrophoretic deposition (EPD). There are many advantages of this technique over other deposition methods such as sputtering, thermal evaporation, doctor-blade etc. For example,[26-28] higher deposition rates can be easily achieved by the EPD method, resulting in a quick deposition in addition to its reproducibility. It is also low cost and an efficient technique with control over thickness and morphology of the films by controlling the applied current or potential. Especially, EPD has a flexibility of depositing films even on uneven shapes and sizes and can be extended to a large scale for commercial applications. Another advantage of this process is that it can be carried out at moderate temperatures thereby reducing the possible deterioration of source and product materials.[26-28]

Herein, we report a rapid microwave-assisted process in aqueous solution for the synthesis of uniform and amorphous precursor compounds for the preparation of pure crystalline $CuInSe_2$ particles by post reduction technique. The precursor powder can be further deposited by EPD followed by a thermal treatment to produce chalcopyrite $CuInSe_2$ thin films. Characterizations of materials accompanied with discussion are given too.

2. Experimental Section

Chemicals: All reactants and solvents were used without further purification. Indium (III) chloride ($InCl_3$, 99.995%) and Ethanol (CH_3CH_2OH, 95%) were both purchased from Acros organic. Acetone (99.9 %) and iodine (99, 8 %) were both purchased from Aldrich. Copper (II) chloride dihydrate ($CuCl_2.2H_2O$ tech., 95%) were purchased from JANSSEN CHIMICA. Sodium Selenite (Na_2SeO_3) was purchased from Fisher Scientific and used as a source of selenium.

Microwave: Microwave syntheses were performed in single mode CEM Discover System operating at 300 W, 2.45 GHz. The sealed solution was heated at different temperature (120 °C, 140 °C, 160 °C and

180 ^{o}C) with 100 W of microwave power for 30 minutes. The reaction is rapidly cooled using high-pressure air following the termination of the reaction.

Synthesis of amorphous precursor compounds: An amorphous precursor compounds, which is a precursor of $CuInSe_2$ particles was prepared by microwave enhanced method in aqueous solution at different reaction temperature and pH value (1, 3, 5 & 7). Further reduction processes of these precursors in the presence of selenium powder were carried out to obtain pure chalcopyrite $CuInSe_2$ particles. For a typical synthesis, 0.5 mmol of Na_2SeSO_3, 0.25 mmol of $InCl_3$ and 0.25 mmol of $CuCl_2.2H_2O$ were added in to 6 mL of deionized water and mixed together. The mixture was stirred and sonicated for 10 minutes respectively. The solution was sealed and heated at different reaction temperature (120,140, 160 & 180 ^{o}C) in 100 W microwave power for 30 minutes. The products were collected after washing with deionized water and ethanol, centrifugation and filtration followed by drying in vacuum at 80 ^{o}C for 6 hrs.

Formation of Crystalline $CuInSe_2$ nanoparticles: Pure crystalline $CuInSe_2$ particles were obtained after reduction of the amorphous precursor compounds in the presence of selenium powder in 2 % H_2-98 % Ar atmosphere at 500 ^{o}C for 3 hrs.

Electrophoretic deposition: The amorphous precursor compounds synthesized by microwave method were added into the mixture of solvents (acetone: ethanol = 3:1 v/v) with a concentration of 10 g powder per liters of solvent. The iodine pellet which is acted as a proton maker was added to the mixture of solvents with the concentration of 0.6 g of iodine per litter of solvents and allows the solution under ultrasonic for 5 hrs to form a stable and uniform suspension. The zeta potentials for the suspension of amorphous precursor compounds versus pH value were shown in Figure S4. At zeta potential where, the solution was highly dispersed with no precipitation and good stability was chosen. A suspension of amorphous precursor compounds with a zeta potential of -30 mV was used for electrophoretic deposition. A molybdenum-coated soda-lime glass (substrate) was employed as working electrode or anode and the stainless steel as counter electrode or cathode with 1 cm distance in between. The electrophoresis deposition was carried out with 20 V, 40 V, 60 V and 80 V of the applied voltage for 90 s.

Formation of Crystalline $CuInSe_2$ films: The crystalline $CuInSe_2$ films were prepared by electrophoretic deposition techniques using the suspension of amorphous precursor compounds followed by thermally annealed at various temperature (500, 550 & 600 ^{o}C) and time (1hr,5hrs & 10 hrs).

Characterization: The images of the as-prepared samples were obtained using a scanning electron microscopy (SEM, JEOL JEM-6500F FESEM) and TEM (Philips Tecnai 20 G2-field emission gun with a maximum acceleration voltage of 200 keV). The elemental compositions of the particle were performed on the Energy Dispersive X-ray spectroscopy **(**EDX elemental analysis, JSM 6500) and Inductively Coupled Plasma mass spectroscopy (ICP, Continuous-Kontron S-35, Germany). X-ray Diffraction measurements (XRD, Rigaku Dmax-B, Japan) were carried out using a Cu Kα Radiation source that was operated at 40 kV and 100 mA. The X-ray diffractogram was obtained at a scan rate of 0.05 deg s^{-1} for 2θ between 20° and 80°. The composition and the oxidation states of the elements in the $CuInSe_2$ films were measureded using X-ray photoelectron spectra (XPS) (PHI, 1600S).

3. Results and Discussion

The images of amorphous precursor compounds synthesized at different temperature were recorded by scanning electron microscopy (SEM) as shown in Figure 1. The image reveals that the powders synthesized at a temperature of 180 ^{o}C have uniform morphology (spherical nanoparticles) with quite uniform size distribution.

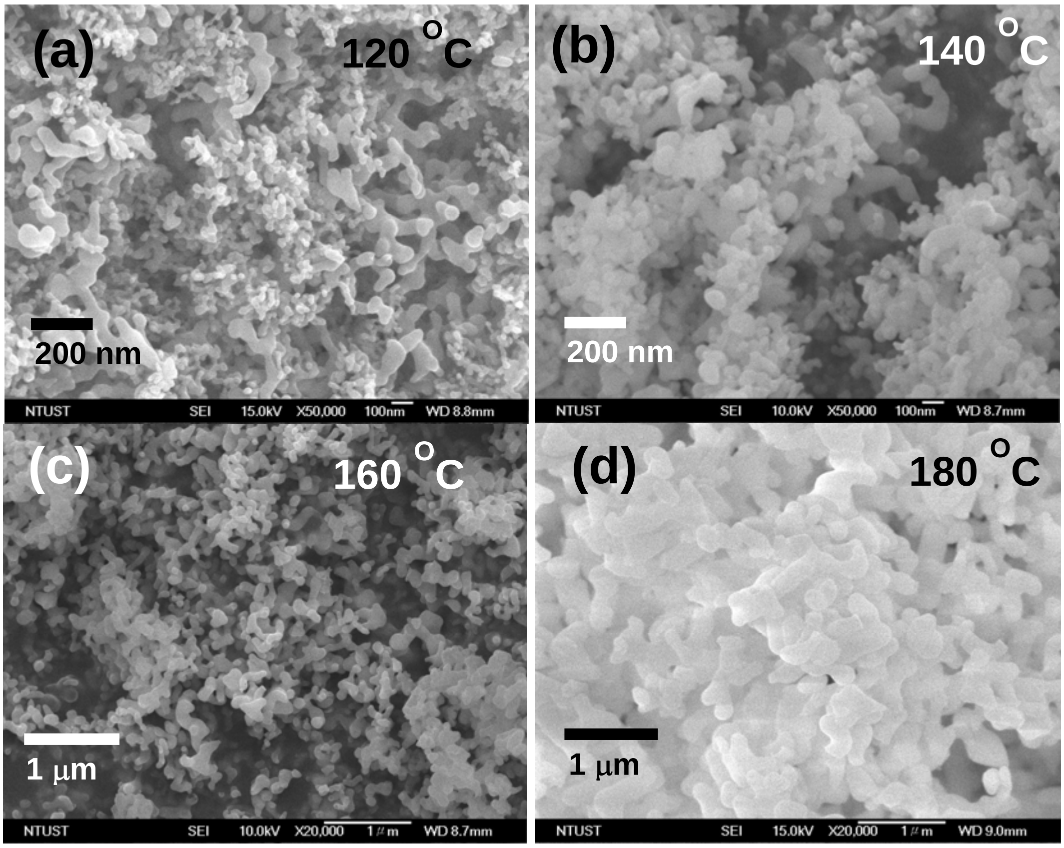

Figure 1. The SEM image of amorphous precursor compounds synthesized by microwave enhanced method in an aqueous solution at different temperature for 30 mins. Scale bars of (a) & (b) 200 mm while (c) & (d) 1 μm.

In order to explain the formation mechanism and its exact stoichiometric composition of the amorphous precursor compounds, the reaction conditions were adjusted and carried out at different temperature and pH values. The results of the elemental compositions of the amorphous precursor compounds synthesized by a microwave enhanced hydrothermal route at various reaction temperatures were obtained using ICP and EDX analyses as summarized in Table 1. The result indicates that the stoichiometric ratio close to the theoretical value was achieved by raising the synthesis temperature to 180 °C. The approximate ratios of the constituent elements in the precursors compounds estimated by both EDX and ICP elemental analyses for Cu: In: Se is 0.99:1:2.19 and 0.94, 1.03, 2.02 respectively, which are close to the stoichiometric value: 1:1:2 at the reaction temperature of 180 °C. Both EDX and

SEM data shows that precursors of high uniformity and best stoichiometric ratio could be achieved by 180 ^{o}C reaction temperatures for 30 mins reaction time with only slightly coarsening of the particle size.

Table 1. Elemental composition of the amorphous precursor compounds synthesized at different reaction temperatures.

Temperature (^{o}C)	EDX Elemental analyses (atomic %)			ICP analysis		
	Cu%	In%	Se%	Cu%	In%	Se%
120	21.87	36.92	21.20	-	-	-
140	32.85	30.81	36.34	-	-	-
160	41.28	21.46	37. 26	-	-	-
180	23.62	23.96	52.42	23.51	25.88	50.59

The pH value of the aqueous solution could also affect the morphology and composition in the hydrothermal synthesis. The results in Table 2 showed that the compounds with better elemental ratios were obtained in an acidic environment (pH 3-5). However, at pH value of 1, the composition become disproportionately. It might be caused by the formation of copper (I) selenide or copper (II) selenide. A uniform morphology of amorphous precursor compounds with best stoichiometry was achieved at a pH value of 5. The images of amorphous precursor compounds synthesized at different pH value were compared in Figure 2.

Table 2. The EDX elemental analysis of amorphous precursor compounds synthesized at 180 °C for 30 mins with different pH values of the solution.

pH value of the reaction	EDX elemental analyses (atomic %)		
	Cu%	In%	Se%
1	4.24	48.02	47.74
3	23.79	26.47	49.74
5	24.25	25.13	50.62
7	31.40	29.16	39.39

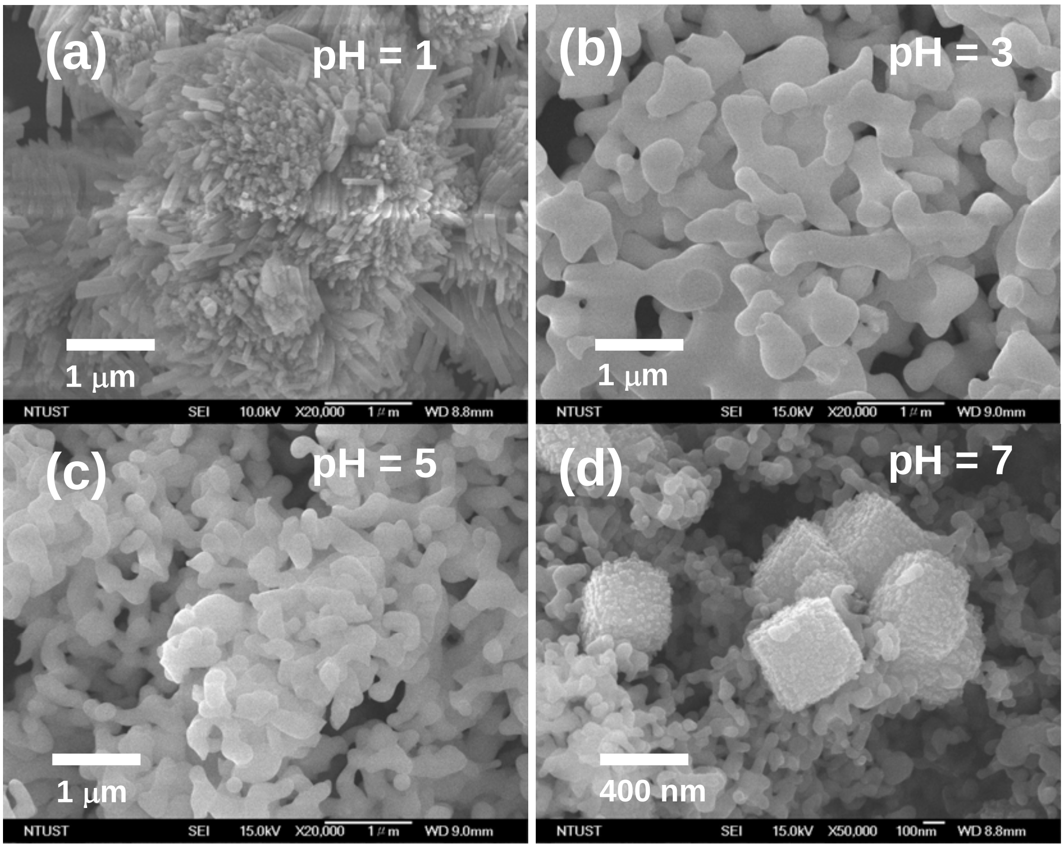

Figure 2. The SEM images of amorphous precursor compounds synthesized by a microwave enhanced method in aqueous solution at different pH values for 180 °C for 30 mins.

For comparison, the amorphous precursor compounds were synthesized by autoclave in 180 °C at different reaction time. The morphology of amorphous precursor compounds that was prepared by autoclave is shown in supporting information (Figure S1). Based on our experimental results, uniform morphology of amorphous precursor compounds synthesized by hydrothermal method using autoclave can be only obtained for at least 10 hrs reaction time. As a result, microwave heating indeed shows a great contribution for low cost, short reaction time and potential for the scale-up production. Finally, the phase and the crystallographic structures of the precursor compounds was determined by X-ray powder diffraction (XRD) and shown in Figure 3. It shows that the precursor compound is amorphous with no evident crystalline phase.

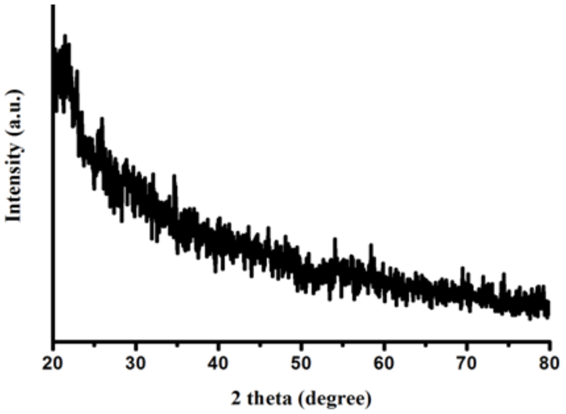

Figure 3. XRD results of amorphous precursor compounds synthesized at 180 °C for 30 mins with pH 5.

Primarily, the amorphous precursor compounds could be reduced to obtain chalcopyrite $CuInSe_2$ particles in the presence of selenium powder at 300 °C, 400 °C and 500 °C in 2 % H_2 and 98 % Ar atmosphere for 3 hrs. The SEM images in Figure 4(a-b) show the morphological features of the chalcopyrite $CuInSe_2$ after reduction of the precursor at 500 °C and the treatment led to the aggregated $CuInSe_2$ powders. The structural evolution after reduction of the precursors at various temperatures was investigated from XRD data (Figure 5). As the reduction temperature increases, three well-defined characteristic peaks at $2\theta = 26^o$, 44^o and 52.5^o, corresponding to the diffraction of the (112), (204, 220), and (116, 312) planes, were clearly identified. This confirmed the formation of typical chalcopyrite phase of $CuInSe_2$ with a tetragonal structure.[29] The reduction temperature was found to be optimal at 500℃ and pure chalcopyrite crystalline structure was produced. Therefore, after initial trials, the reduction condition was set to be 500 °C in 2 % H_2 and 98 % Ar atmosphere for 3 hrs. However, the elemental ratio of $CuInSe_2$ powders measured by EDX deviated slightly from its theoretical value, as seen in Figure 4 (b).

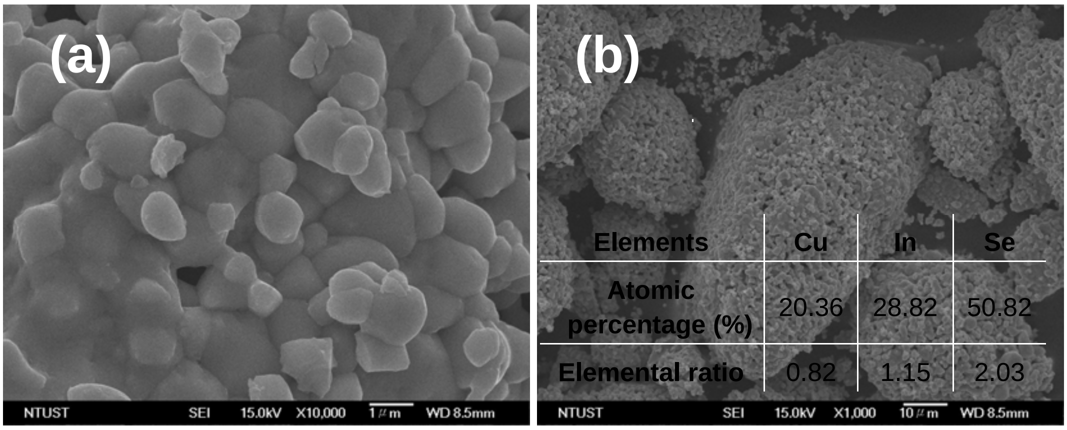

Elements	Cu	In	Se
Atomic percentage (%)	20.36	28.82	50.82
Elemental ratio	0.82	1.15	2.03

Figure 4. SEM images (a & b) and EDX results of $CuInSe_2$ particles after reduction at 500 °C for 3 hrs.

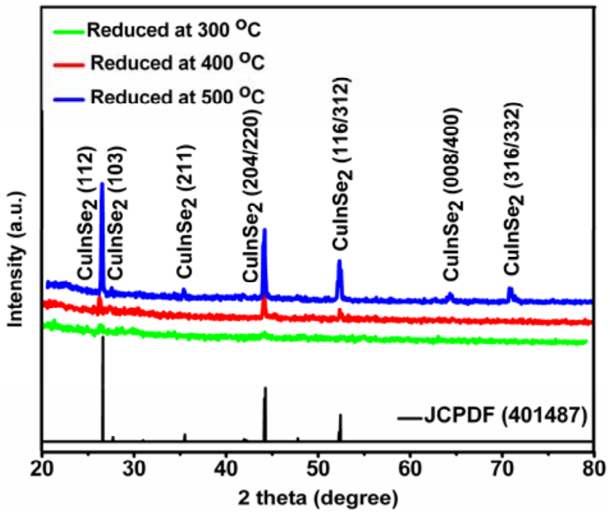

Figure 5. XRD results of $CuInSe_2$ particles prepared by reduction of amorphous precursor at different temperatures.

To prove the processability of the as-prepared amorphous precursor, electrophoretic deposition technique was employed to prepare the absorber layer for thin film solar cells. $CuInSe_2$ films were produced by electrophoretic deposition of the as-prepared amorphous precursor on a molybdenum-coated glass followed by thermal reduction. As seen in Figure 6, pure crystalline $CuInSe_2$ phases could be obtained after thermal reduction of the films. Three well-defined characteristic peaks at $2\theta = 26^o$, 44^o and 52.5^o, corresponding to the diffraction of the (112), (204, 220), and (116, 312) planes, were clearly identified. This confirmed the formation of typical chalcopyrite phase of $CuInSe_2$ with a tetragonal structure.[29] The diffraction peaks for $MoSe_2$ and Mo appeared because the $CuInSe_2$ film was deposited on the Molybdenum coated soda-lime glass substrate as a result the reaction of the Mo glass with porous film during selenization may lead the formation of $MoSe_2$ while Mo peaks from the substrate (a molybdenum coated soda-lime glass). The trend of grain sizes for the deposited films was not obvious, maybe due to the small difference among the annealing conditions. The SEM images of $CuInSe_2$ films fabricated by electrophoretic deposition followed by annealing at 600℃ for 1hr, 5 hrs and 10 hrs are shown in Figure 7(a)-(c). Figure 7(d) shows the representative cross-sectional image of $CuInSe_2$ films fabricated by electrophoretic deposition followed by annealing at 600℃ for 10 hrs. Based on the SEM cross-section measurement, the thickness of $CuInSe_2$ films prepared by electrophoretic deposition at different applied voltage and deposition times is shown in Figure S2. The surface morphologies of the films are porous yet uniform. Although there are still engineering work remaining to optimize the whole process, the results demonstrates that it is viable approach using the as-prepared amorphous precursor compounds to produce the crystalline $CuInSe_2$ particles (via post reduction) or films (via the electrophoretic deposition) for solar cell applications.

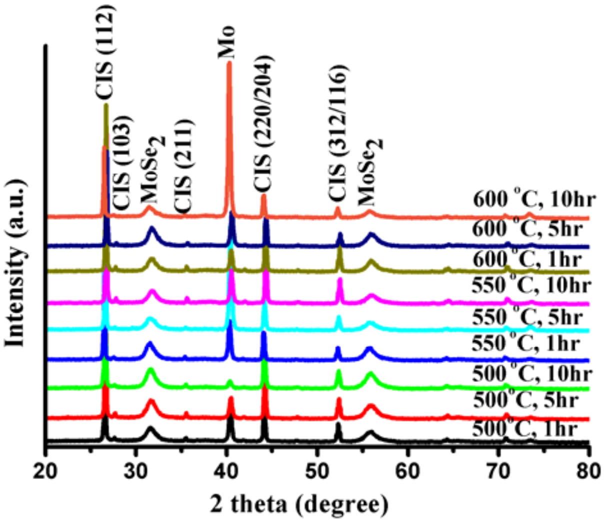

Figure 6. XRD results of $CuInSe_2$ films fabricated by electrophoretic deposition. The films were annealed at 500, 550, and 600℃ and each annealing temperature was maintained for 1, 5, and 10 hrs separately.

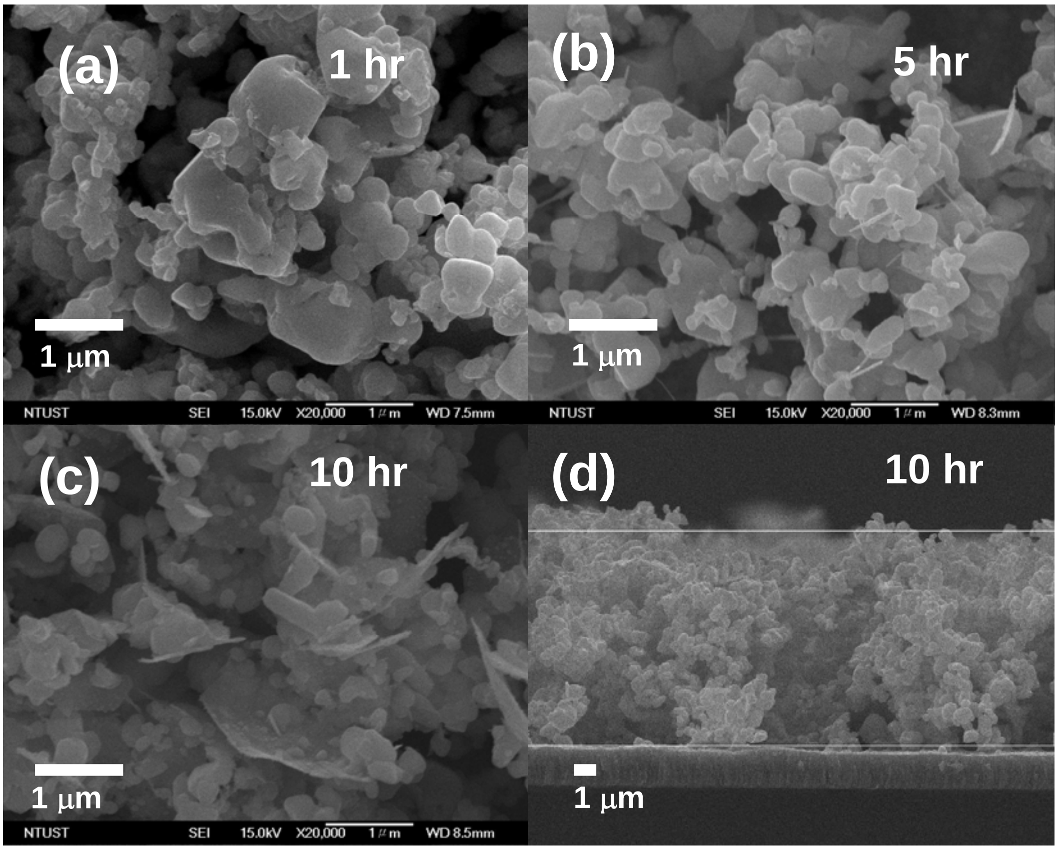

Figure 7. The SEM images of $CuInSe_2$ films fabricated by electrophoretic deposition using the as-prepared amorphous precursor compound followed by annealing at 600℃ for (a)1 hr, (b) 5 hrs and (c) 10 hrs with its representative SEM cross section (d).

Overall speaking, the proposed route involves more processing steps, i.e. film formation and thermal treatment, than a direct synthesis of chalcopyrite nanoparticles. However, it provides an alternative for better control over the composition and crystal growth, which are critical to the conversion efficiency of thin film solar cells. The application of amorphous precursor is expected to bring substantial benefits and flexibility in forming the absorber layer of $CuInSe_2$ and other similar chalcopyrite compounds, provided that the film formation and annealing conditions can be further optimized. The TEM (Figure S3a), HRTEM image (Figure S3b) and the corresponding selected area electron diffraction (SAED) (Figure S3c) for the as-deposited $CuInSe_2$ films via electrophoretic deposition of the amorphous precursor compounds followed annealing at 600 °C for 10 hrs. The lattice fringes in the HRTEM images (Figure S3b) confirms that the $CuInSe_2$ films formed from the amorphous precursors are purely crystalline. Furthermore, in the HRTEM image of $CuInSe_2$ (in Fig. S3b), the observed d-spacing is about 0.3 nm and is complied with the (1 1 2) lattice spacing of chalcopyrite $CuInSe_2$ nanoparticles. The crystallographic diffraction patterns (Fig. S3c) possess several rings composed many discrete spots, and the rings match well with (1 1 2), (2 2 0)/ (2 0 4), and (1 1 6)/ (3 1 2) reflections of the tetragonal $CuInSe_2$. [18]

The XPS data for the as-deposited $CuInSe_2$ films are shown in Figure 7. The binding energy of Cu $2p_{3/2}$ was 932.45 eV which indicates copper was reduced from Cu^{2+} (binding energy centered at 942 eV) to Cu^{+} corresponding to binding in $CuInSe_2$. The FWHM for peaks Cu $2p_{3/2}$ and Cu $2p_{1/2}$ were 1.9 and 2.3 eV, respectively, and these are also in good agreement with the reported values for Cu^{+}.[30-32] The oxidation state of Cu, In and Se are found to be +1, +3 and -2 respectively.

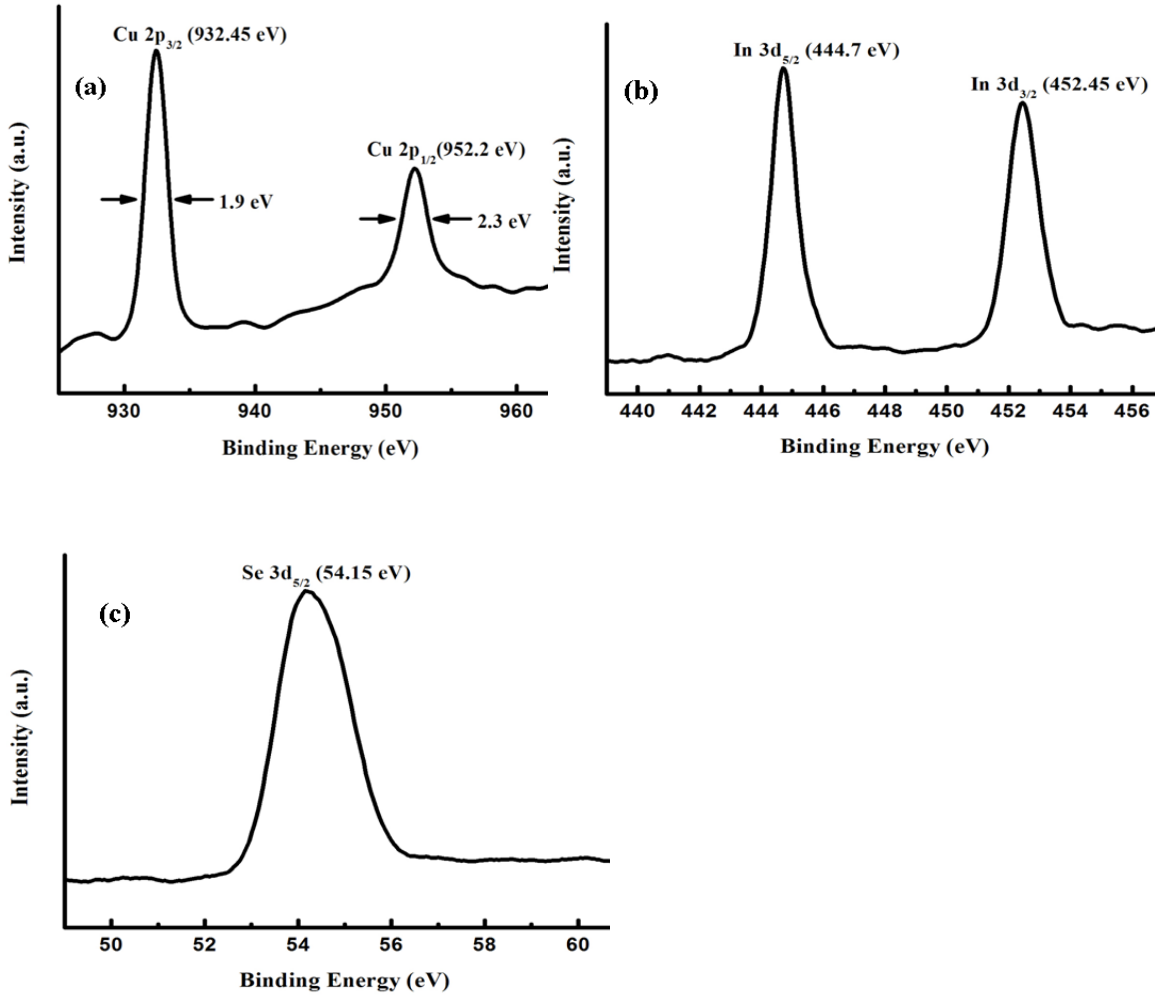

Figure 8. XPS spectra of an as-deposited CuInSe2 film for Cu 2p (a), In 3d (b) and Se 3d (c) signals

Reaction mechanisms: Although intermediate products such as In_2Se_3 and CuSe have been reported in the XRD patterns of $CuInSe_2$ particles,[33] these intermediate products did not appear in amorphous precursor compounds, as seen in the XRD result in Figure 3. This suggested that all the intermediate products in the preparation of precursor compounds were amorphous. Therefore, based on our current experimental results and literature, we proposed the following possible reaction mechanism for the formation of amorphous compounds and its transformation to crystalline $CuInSe_2$.

1. $Na_2SeO_3 + CuCl_2 \rightarrow CuSeO_3 + NaCl$
2. $Na_2SeO_3 + InCl_3 \rightarrow In_2(SeO_3)_3 + NaCl$
3. $CuSeO_3 + In_2(SeO_3)_3 \rightarrow CuInSe_2O_5$ + by products

4. $CuInSe_2O_5 \xrightarrow{\text{Reduction in } H_2\text{(2 \%)-Ar (98 \%) in Se}}$ Crystalline $CuInSe_2$ particle + O_2
5. $CuInSe_2O_5 \xrightarrow{\text{Electrophoretic deposition}} \xrightarrow{\text{Annealing}}$ Crystalline $CuInSe_2$ film + O_2

Both intermediate products, $CuSeO_3$ and $In_2(SeO_3)_3$ were amorphous.[34] No characteristic peaks of other impurities, such as Se or Cu_2Se, were detected in the XRD pattern. Under this hydrothermal synthesis conditions, the water was used as a reducing agent[34] to release Cu^{+1} and Se^{-2} as ethanol reduces Cu^{+2} to Cu^{+1}.[35] Moreover, it may be easier to reduce $CuSeO_3$ compared to $In_2(SeO_3)_3$.[34] From the EDX and ICP data (in Table 1 & 2), the stoichiometric composition of Cu, In and Se in the as prepared amorphous precursors compounds were 1:1:2. This result suggested that the final precursor compounds were diselenite as seen in step 3. The as-prepared amorphous precursor compounds were then transformed to crystalline $CuInSe_2$ (step 4 &5).

4. Conclusions

In this study**,** we have shown that a uniform structure of amorphous precursor compounds can be successfully synthesized by microwave enhanced process in aqueous solution at a pH of 5 under 180 °C for 30 mins, which is a great improvement in reducing the reaction time and temperature. Pure chalcopyrite $CuInSe_2$ particles with better stoichiometry is attainable by post reduction of the amorphous precursor compounds with selenium powder in an atmosphere of 2% H_2 and 98% Ar at 500 °C for 3 hrs. The morphological and compositional features of amorphous precursor compounds and $CuInSe_2$ particles were characterized by XRD, SEM, and EDX elemental analysis. $CuInSe_2$ particles prepared by the proposed microwave assisted method followed by reduction give the ideal stoichiometry and purity. Microwave assisted hydrothermal method proves to be a convenient way to control the morphology and crystallinity of the products. The obtained amorphous compound was demonstrated to fabricate uniform $CuInSe_2$ thin film for solar cell applications by the electrophoretic deposition. Overall, the integrated concept of formulating a precursor with designated composition and the following reduction and deposition processes offers a viable, simplified and economical option to current dry processes. Using the as-prepared amorphous compound as a precursor for the preparation of $CuInSe_2$ films or powders, it gives a better control over the crystallinity of $CuInSe_2$ via manipulating deposition and reduction parameters than a one-step production $CuInSe_2$ crystal. Although the concentration of reactants and reduction temperature are supposed to be responsible for the formation of amorphous compound and its transformation to crystalline $CuInSe_2$ respectively, further investigation on the formation mechanism of amorphous compound and its transformation to crystalline $CuInSe_2$ is underway. The optimized approach can be also applied to other similar materials and their industrial applications.

Acknowledgment

We gratefully acknowledge the financial support from the Ministry of Education (MOE) Top University Project-102H451401 and facilities from the National Taiwan University of Science and Technology (NTUST), Taiwan.

5. References

1. G. Hodes and D. Cahen, *Solar Cells* 1986, **16**, 245–254.
2. H. Metzner, A. Dietz, M. Gossla, U. Reislohner, N. Rega, S. Siebentritt, T. Hahn and W. Witthuhn, *J. Phys. Chem. Solids* 2005, **66**, 1940–1943.
3. J. Yang, Z. Jin, T. Liu, C. Li and Y. Shi, *Sol. Energy Mater. Sol. Cells* 2008, **92**, 621–627.
4. H. Matsushita, T. Ochiai, K. Mikajiri and A. J. Katsui, *J. Phys. Chem. Solids* 2005, **66**, 1937–1939.
5. R. Trykozko, R. Bacewicz and J. Filipowicz, *Solar Cells* 1986, **16**, 351 – 356.
6. J. Qiu, Z. Jin, W. B. Wu and L.-X. Xiao, *Thin Solid Films*, 2006, **510**, 1-5.
7. A. D. Compaan, *Sol. Energy Mater. Sol. Cells* 2006, **90**, 2170.
8. Y. Sudo, S. Endo and T. Irie, *Jpn. J. Appl. Phys.* , 1993, **32**, 1562.
9. S. Isomura, T. Kariya and S. Shirakata, *Cryst. Res. Technol.* , 1996, **31**, 523.
10. M. Krunksa, V. Miklib, O. Bijakinaa, H. Rebanea, A. Merec, T. Varemaa and E. Mellikov, *Thin Solid Films*, 2000, **361**, 61.
11. J. A. Thornton, T. C. Lommasson, H. Talieh and B.-H. Tseng, *Solar Cells*, 1988, **24**, 1–9.
12. E. R. Don, R. Hill and G. J. Russell, *Solar Cells*, 1986, **16**, 131–142.
13. J. W. Park, G. Y. Chung, B. T. Ahn, H. B. Im and J. S. Song, *Thin Solid Films* 1994, **245**, 174.
14. C. C. Landry, J. Lockwood and A. R. Barron, *Chem. Mater.*, 1995, **7**, 699–706.
15. B. Li, Y. Xie, J. Huang and Y. Qian, *Adv. Mater.*, 1999, **11**, 1456-1459.
16. X. Gou, F. Cheng, Y. Shi, L. Zhang, S. Peng, J. Chen and P. Shen, *J. Am. Chem. Soc.*, 2006, **128** 7222-7229.
17. C. Burda, X. Chen, R. Narayanan and M. A. El-Sayed, *Chem Rev.* , 2005, **105**, 1025-1102.
18. R. Pazik, R. J. Wiglusz and W. Strek, *Mater. Res.Bull.* , 2009, **44**, 1328–1333.
19. P. Raveendran, J. Fu and S. L. Wallen, *J. Am. Chem. Soc.*, 2003, **125**, 13940-13941.
20. H. Hayashi and Y. Hakuta, *Materials*, 2010, **3**, 3794-3817.
21. F. I. Pires, E. Joanni, R. Savu, M. A. Zaghete, E. Longo and J. A. Varela, *Mater. Lett.*, 2008, **62**, 239–242.
22. D. W. Ayele, H.-M. Chen, W.-N. Su, C.-J. Pan, L.-Y. Chen, H.-L. Chou, J.-H. Cheng, B.-J. Hwang and J.-F. Lee, *Chem. Eur. J.* , 2011, **17**, 5737 – 5744.
23. Y. Jin, C. An, K. Tang, L. Huang and G. Shen, *Mater. Lett.* , 2003, **57**, 4267–4270.
24. Y. Groisman and A. Gedanken, *J. Phys. Chem. C* 2008, **112**, 8802–8808.
25. B.-J. Hwang, T.-H. Yu, M.-Y. Cheng and R. Santhanam, *J. Mater. Chem.* , 2009, **19**, 4536-4544.
26. I. Shih, S. K. Zhang and C. X. Qiu, *Solar Cells*, 1986, **16** 283 - 287.
27. E. W. Williams, K. Jones, A. J. Griffiths, D. J. Roughley, J. M. Bell, J. H. Steven, M. J. Huson, M. Rhodes and T. Costich, *Solar Cells*, 1979, **1**, 357 - 366.
28. G.-S. Kim, H.-K. Seo, V. P. Godble, Y.-S. Kim, O.-B. Yang and H.-S. Shin, *Electrochem. Commun.*, 2006, **8**, 961–966.
29. H. Chen, S.-M. Yu, D.-W. Shin and J.-B. Yoo, *Nanoscale Res. Lett.*, 2010, **5**, 217–223.
30. Y. Min, G. D. Moon, J. Park, M. Park and U. Jeong, *Nanotechnology*, 2011, **22**, 465604-465604.
31. L. D. Partain, R. A. Schneider, L. F. Donaghey and P. S. McLeod, *J. Appl. Phys.*, 1985, **57**, 5056.
32. Z. Suo, E. Y. Ma, H. Gleskova and S. Wagner, *Appl. Phys. Lett.* , 1999, **74**, 1177.
33. W. K. Kim, S. Kim, E. A. Payzant, S. A. Speakman, S. Yoon , R. M. Kaczynski, R. D. Acher, T. J. Anderson, O. D. Crisalle, S. S. Li and V. Craciun, *J. Phys. Chem. Solids,* , 2005, **66**, 1915-1919.
34. M. Wang, S. K. Batabyal, Z. Li, D. Li, S. G. Mhaisalkar and Y. M. Lam, *RSC Adv.* , 2013, **3**, 9829-9834.
35. Y. Sun, Y. Zhang, H. Wang, M. Xie, K. Zong, H. Zheng, Y. Shu, J. Liu, H. Yan, M. Zhu and W. Lau, *J. Mater. Chem. A*, 2013, **1**, 6880-6887.